Diffusion-Based Distributed Wave-Domain Active Noise Control With Convex Sum of Non-Convex Quadratic Costs

Mengfei Zhang, Yuchen Dong, Jie Chen, Cédric Richard

Diffusion-based Distributed Wave-Domain Active Noise Control with Convex Sum of Non-Convex Quadratic Costs

Mengfei Zhang, *Student Member, IEEE*, Yuchen Dong, *Student Member, IEEE*, Jie Chen, *Senior Member, IEEE*, and Cédric Richard, *Senior Member, IEEE*

***Abstract*—Active noise control (ANC) in the wave-domain has been widely used to perform noise cancellation in large spatial areas with time-varying acoustic characteristics. Most of existing works on ANC focus on centralized strategies where the residual signals from all microphones are required for performing each estimate update. Nonetheless, as the number of speakers and microphones increases, the centralized strategy might encounter challenges related to flexibility and scalability. The aim of this work is to introduce a distributed wave-domain ANC method based on a convex sum of non-convex quadratic costs to spread the computational load amongst nodes to overcome these issues. In order to minimize the ANC cost, we consider a group diffusion adaptation strategy, where the errors measured at each node, and the driving signal estimated at each node, involve those nodes individually and their neighbors. As a result, additional nodes with microphones or speakers can be easily integrated into the system, and each node can process with low computational complexity. Comparing the proposed algorithm to its centralized and distributed counterparts, we evaluate the algorithm's efficacy in various environments.**

***Index Terms*—Distributed optimization, active noise control, non-convex decomposition, distributed networks, diffusion adaptation.**

I. Introduction

BECAUSE noise can cause permanent damage to auditory organs and interfere with sleep, recreation, and work, environmental noise represents a serious global health concern. Many epidemiological studies have linked ambient noise to a variety of health issues, such as myocardial infarction, arterial hypertension, and stroke [1]. Among other solutions, active noise control (ANC) permits a noise cancellation zone to control secondary sound sources for cancelling the original noise via destructive interference [2]. This strategy has been successfully applied, for instance, in vehicles [3], [4].

Adaptive algorithms have been widely studied as tools to perform noise cancellation over time-varying environments. They can operate in the frequency domain [5], time domain [6] or wave domain [7]. Wave-domain-based methods, which minimize the sum of squared harmonic coefficients over the entire spatial region, have shown improved spatial consistency. Nonetheless, they need to collect data from all sensors and process them with a centralized approach. This prevents their use over large spatial areas because of the high communication and computation costs [8]. In applying the wave-domain ANC methods in practical vehicles [3], [4], it is crucial to consider adjusting the sensor count and position to accommodate various application scenarios. This necessitates that the system be more scalable. Then, to tackle these difficulties, it has appeared reasonable to explore ways of implementing distributed strategies. Wireless acoustic sensor networks (WASN) have contributed to significant breakthroughs in distributed methods for ANC as they allow to distribute the computation load over all nodes [8]–[10]. In [9], the authors introduce an incremental strategy into ANC systems. Nevertheless, data need to travel from one node to the next until browsing the whole network. On the other hand, the effectiveness of diffusion methods introduced in [11]–[13] has motivated researchers to implement this strategy in the wave domain, leading to diffusion-based ANC [8], [10]. Nevertheless, the performance of the diffusion-based algorithm introduced in [10] is hindered by an approximate formulation of the centralized problem required by the distributed strategy. The distributed minimum variance distortionless response (MVDR) problem is formulated in [14] by splitting the global quadratic cost into a convex sum of non-convex local costs [15]. A similar non-convex decomposition is considered in [16]. The optimization problem is addressed with the Primal-Dual Method of Multipliers. The effectiveness of these distributed strategies for minimizing non-convex decompositions of global quadratic costs definitely offers new perspectives to address ANC in a distributed manner.

The objective of this paper is to address the ANC problem in the wave domain with a distributed strategy by considering a non-convex decomposition of the centralized quadratic criterion. The group diffusion least mean square algorithm [17] is used so that each node can estimate its own driving signal parameters based on information sharing with its neighbors. Simulations are conducted to validate the proposed algorithm over free and reverberant fields.

II. Problem formulation

We shall now address the ANC problem over a spatial area illustrated in Figure 1(a). Assume, for the sake of generality, that the noise cancellation zone is delimited by a circular area of radius R_1 while the noise source is locate beyond this area, and the secondary sources are generated by a circular array of loudspeakers with Q elements and radius R_2, where $R_2 > R_1$.

The work of M. Zhang was supported partly by the China Scholarship Council and partly by the Innovation Foundation for Doctor Dissertation of Northwestern Polytechnical University.

M. Zhang, Y. Dong and J. Chen are with School of Marine Science and Technology, Northwestern Polytechinical University, Xi'an, 710072, China (e-mail: {zhangmengfei, dyc311}@mail.nwpu.edu.cn, dr.jie.chen@ieee.org). Cédric Richard is with Université Côte d'Azur, Nice, France (e-mail: cedric.richard@unice.fr).

A feedback control strategy is employed to cancel the noise in the rejection area [18]. In the zone of noise cancellation, the residual signals shall be measured at free position $\boldsymbol{r} = (r, \theta_{\boldsymbol{r}})$. Within the control region $\boldsymbol{r} \leq R_1$, the primary noise wave field $v(\boldsymbol{r}, k_f)$ observed at $\boldsymbol{r}$ is approximated as the sum of a finite number of modes using the cylindrical harmonic wave function expansion:

$$v(\boldsymbol{r}, k_f) \approx \sum_{\rho=-S}^{S} \beta_\rho(k_f) \mathcal{J}_\rho(r k_f) \exp(j\rho\theta_{\boldsymbol{r}}), \tag{1}$$

where the wave number is defined as $k_f \triangleq 2\pi f/c$ with frequency f and sound speed c, an integer number $\rho \in [-S\ S]$ is the order of the Bessel function $\mathcal{J}_\rho(\cdot)$ with $S = \lceil r k_f \rceil$ [19], and $\beta_\rho(k_f)$ is the coefficients of the primary noise field in wave-domain.

Likewise, the loudspeaker array generates the secondary sound field $s(\boldsymbol{r}, k_f)$ at $\boldsymbol{r}$ as [20]:

$$s(\boldsymbol{r}, k_f) \approx \sum_{\rho=-S}^{S} \gamma_\rho(k_f) \mathcal{J}_\rho(r k_f) \exp(j\rho\theta_{\boldsymbol{r}}), \tag{2}$$

where the wave-domain coefficients $\gamma_\rho(k_f)$ are given by:

$$\gamma_\rho(k_f) = \sum_{q=1}^{Q} d_q(k_f)\, T_{\rho,q}(k_f), \tag{3}$$

with the q-th loudspeaker driven by the signal $d_q(k_f)$. For sound propagation in free field, the coefficients $T_{\rho,q}(k_f)$ of the acoustic transfer function (ATF) in the wave domain are calculated as follows:

$$T_{\rho,q}(k_f) = \frac{j}{4} \mathcal{H}_\rho^{(2)}(k_f \|\boldsymbol{r}_q\|) \exp(j\rho\theta_{\boldsymbol{r}_q}), \tag{4}$$

where the ρ-th order of Hankel function in the second kind is denoted as $\mathcal{H}_\rho^{(2)}(\cdot)$ and $\boldsymbol{r}_q$ is the location of the q-th source. Based on (1) and (2), the residual signals at $\boldsymbol{r}$ are given by:

$$\begin{aligned} e(\boldsymbol{r}, k_f) &= v(\boldsymbol{r}, k_f) + s(\boldsymbol{r}, k_f) \\ &\approx \sum_{\rho=-S}^{S} \underbrace{(\beta_\rho(k_f) + \gamma_\rho(k_f))}_{\alpha_\rho(k_f)} \mathcal{J}_\rho(r k_f) \exp(j\rho\theta_{\boldsymbol{r}}), \end{aligned} \tag{5}$$

with $\alpha_\rho(k_f)$ the error sound field decomposition coefficients.

Using a block-wise operation, we transform the microphone signal into the time-frequency domain and consequently represent it as the wave-domain coefficients, based on (5). Wave-domain ANC involves designing the loudspeaker driving signals $s(\boldsymbol{r}, k_f)$ to cancel $v(\boldsymbol{r}, k_f)$ in the control zone. Based on signal propagation models (1) and (2), for notational simplicity, we express the residual sound field coefficients in the wave domain at a given time index i in matrix form by removing the wave number k_f as:

$$\boldsymbol{\alpha}(i) = \boldsymbol{\beta}(i) + \boldsymbol{\gamma}(i) = \boldsymbol{\beta}(i) + \boldsymbol{T}\boldsymbol{d}(i), \tag{6}$$

where $\boldsymbol{\alpha}(i)$, $\boldsymbol{\beta}(i)$ and $\boldsymbol{\gamma}(i)$ are vectors of length $2S+1$ with entries $\alpha_\rho(i)$, $\beta_\rho(i)$ and $\gamma_\rho(i)$, respectively, $\boldsymbol{T}$ is a matrix of size $(2S+1)\times Q$ with entries $T_{\rho,q}(k_f)$ and $\boldsymbol{d}(i)$ is the Q-length vector with entries $d_q(k_f)$.

Based on (5), the residual sound field coefficients at each iteration i (the i-th time block) can be rewritten as:

$$\boldsymbol{\alpha}(i) = \boldsymbol{B}^{-1}\boldsymbol{F}\boldsymbol{e}(i), \tag{7}$$

with $\boldsymbol{e}(i)$ the vector of errors measured by the N microphones located at $\boldsymbol{r}_n = (R_1, \theta_n)$ with $n = 0, \ldots, N-1$, and the diagonal matrix $\boldsymbol{B} = \mathrm{diag}\{\mathcal{J}_{-S}(R_1 k_f), \ldots, \mathcal{J}_S(R_1 k_f)\}$ of corresponding Bessel function coefficients. In this expression, $\boldsymbol{F}$ denotes the $(2S+1)\times N$ complex matrix with (ρ, n)-th entry defined as: $F_{\rho,n} = \frac{1}{N} e^{-j(-S+\rho-1)\theta_n}$.

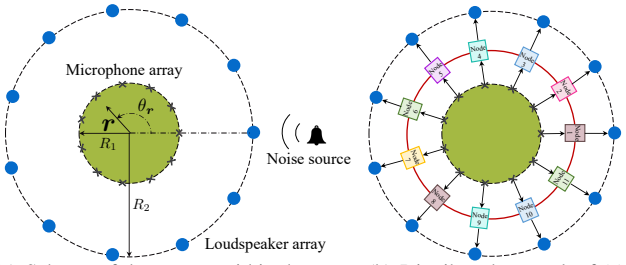

(a) Schema of the system within the control field (green area), equipped with a circular array of microphones with radius R_1 and a circular array of loudspeakers with radius R_2.

(b) Distributed network of 11 nodes, where each node possesses 1 microphone and 1 speaker.

Fig. 1: The simulated ANC System.

The cost function for minimizing residual field energy is the sum of the squared coefficients of the residual signal in the wave domain [21]:

$$J(\boldsymbol{\alpha}) = \sum_{\rho=-S}^{S} |\alpha_\rho(i)|^2 = \boldsymbol{\alpha}^{\mathrm{H}}(i)\boldsymbol{\alpha}(i), \tag{8}$$

where $(\cdot)^{\mathrm{H}}$ denotes the conjugate transpose. Note that $J(\boldsymbol{\alpha})$ is strictly convex with respect to $\boldsymbol{\alpha}(i)$. As shown in the next section, this property is no longer valid locally when $J(\boldsymbol{\alpha})$ is distributed over the nodes of the network.

III. Distributed wave-domain ANC based on convex sum of non-convex local costs

Consider a network with a set $\mathcal{N}$ of N nodes interconnected by a set of edges $\mathcal{E}$ supporting some ANC architecture. If an edge exists between two nodes k and ℓ, we say $(k, \ell) \in \mathcal{E}$. All nodes are considered self-connected. The set of nodes having an edge with a node k defines its neighbourhood $\mathcal{N}_k$.

In the ANC architecture, each node is specified as a module having one or more microphones and loudspeakers, as well as a processor with communication and computational capabilities. As illustrated in Figure 1(b), for simplicity, we shall consider the single-channel situation in which each node k is equipped with a single microphone and a single loudspeaker. This means that $Q = N$. To reformulate the ANC problem in a distributed manner, it can be checked that cost (8) can also be written as follows, where the time index i is omitted for simplicity:

$$J(\boldsymbol{d}) = \boldsymbol{d}^{\mathrm{H}}\boldsymbol{R}\boldsymbol{e} + \boldsymbol{v}^{\mathrm{H}}\boldsymbol{R}^{\mathrm{H}}\boldsymbol{d} + \lambda, \tag{9}$$

where $\boldsymbol{d}$ is the N-length vector whose entry d_k is the driving signal of the loudspeaker at node k, $\boldsymbol{v}$ is the N-length vector whose entry v_k defined in (1) is the observation provided by the microphone at node k, $\boldsymbol{R} \triangleq \frac{1}{N}\boldsymbol{T}^{\mathrm{H}}\boldsymbol{B}^{-1}\boldsymbol{F}$ and $\lambda \triangleq \|\boldsymbol{\beta}\|^2$. Note that $\boldsymbol{R}$, $\boldsymbol{v}$ and λ are independent of the driving vector $\boldsymbol{d}$, while $\boldsymbol{e} = \boldsymbol{v} + N\boldsymbol{F}^{\mathrm{H}}\boldsymbol{B}\boldsymbol{T}\boldsymbol{d}$ depends on $\boldsymbol{d}$. Criterion (9) is thus quadratic (and strictly convex) with respect to $\boldsymbol{d}$. As shown hereafter, formulation (9) simplifies local gradients calculation.

A. Problem Reformulation

Following the decomposition principle introduced in [14] for the first two terms depending on $\boldsymbol{R}$ in (9), the cost $J(\boldsymbol{d})$

in (9) is equivalently expressed as the sum of local costs $J_k(\boldsymbol{d}_k)$:

$$\min J(\boldsymbol{d}) = \sum_{k=1}^{N} J_k(\boldsymbol{d}_k) \tag{10a}$$

$$\text{s.t.} \quad \boldsymbol{C}_{k\ell}\,\boldsymbol{d}_k + \boldsymbol{C}_{\ell k}\,\boldsymbol{d}_\ell = \boldsymbol{0}, \quad \forall (k,\ell) \in \mathcal{E}, \tag{10b}$$

with

$$J_k(\boldsymbol{d}_k) = \boldsymbol{d}_k^{\mathrm{H}}\,\boldsymbol{Z}_k\,\boldsymbol{e}_k + \boldsymbol{v}_k^{\mathrm{H}}\,\boldsymbol{Z}_k^{\mathrm{H}}\,\boldsymbol{d}_k + \frac{\lambda}{N} \tag{11}$$

where $\boldsymbol{d}_k \in \mathbb{C}^{|\mathcal{N}_k|}$ denotes the sub-vector of $\boldsymbol{d}$ whose entries are the driving signals at all nodes in $\mathcal{N}_k$, that is, node k itself and its neighbors. We write:

$$\boldsymbol{d}_k \triangleq [\boldsymbol{d}]_{\mathcal{N}_k}, \tag{12}$$

where $[\cdot]_{\mathcal{I}}$ denotes the entries of the vector or matrix argument of the operator indexed by set $\mathcal{I}$. Similarly, $|\mathcal{N}_k|$-length vectors $\boldsymbol{v}_k$ and $\boldsymbol{e}_k$ follow the same construction rule as $\boldsymbol{d}_k$, that is,

$$\boldsymbol{v}_k \triangleq [\boldsymbol{v}]_{\mathcal{N}_k} \qquad \boldsymbol{e}_k \triangleq [\boldsymbol{e}]_{\mathcal{N}_k} \tag{13}$$

Let us denote by $\boldsymbol{A}$ the adjacency matrix defined as: $A_{k\ell} = 1$ if $(k,\ell) \in \mathcal{E}$ including $k = \ell$, and 0 otherwise. In (11), matrix $\boldsymbol{Z}_k$ is defined as:

$$\boldsymbol{Z}_k \triangleq [(\boldsymbol{A}^2)^{\circ -1} \circ \boldsymbol{R}]_{\mathcal{N}_k}, \tag{14}$$

with $(\cdot)^{\circ -1}$ the Hadamard (element-wise) inverse of its matrix argument, here $\boldsymbol{A}^2$, and $\circ$ the Hadamard product. Note that local costs $J_k(\boldsymbol{d}_k)$ are quadratic but no longer convex because of the Hadamard inverse operator in the definition of matrix $\boldsymbol{Z}_k$. Linear equality constraints in (10b) maintain the consistency between all entries, say, of $\boldsymbol{d}_k$ and $\boldsymbol{d}_\ell$ with $\ell \in \mathcal{N}_k$, when these entries are related to a same node. Accordingly, possible entries for matrices $\boldsymbol{C}_{k\ell}$ and $\boldsymbol{C}_{\ell k}$ are -1, 0 and 1.

In the next section, we shall devise a diffusion algorithm for solving problem (10) in a distributed manner. We initially introduced the Group diffusion least mean square (LMS) in [17] to address problems that differ from (10). Interestingly, it is used here because it allows us to address linear constraints in a convenient way.

B. Distributed optimization with Group Diffusion Adaptation

Consider using a diffusion LMS strategy [22] for minimizing the global cost (10). The network estimates $\boldsymbol{d}$ through the collaboration of all nodes with their neighbors, and uses it to control secondary sound sources for ANC task. That is, at each time instant i, a local parameter vector $\boldsymbol{d}_{k,i}$ of length $|\mathcal{N}_k| \times 1$ is estimated at each node k. It is defined as:

$$\boldsymbol{d}_{k,i} = \mathrm{col}\{d_{\ell,k,i}\}_{\ell \in \mathcal{N}_k} \quad \forall k = 1, \ldots, N. \tag{15}$$

where $\mathrm{col}\{\cdot\}$ stacks its scalar arguments on top of each other, and $d_{\ell,k,i}$ is the estimate at node k and time index i of the driving signal coefficient intended for loudspeaker ℓ.

Standard diffusion LMS originally defined in [22] cannot be used to address problem (10) because it aims to collaboratively estimate a single parameter vector which is common to all nodes. On the contrary, with definition (12), parameter vectors $\boldsymbol{d}_k$ differ structurally because each one contains local driving signal estimates for loudspeakers in its neighborhood $\mathcal{N}_k$. However, consistency conditions (10b) point out the need for entries $\{d_{\ell,k,i}\}_{k \in \mathcal{N}_\ell}$ to reach a consensus. Indeed, they are all estimates of the same driving signal parameter $d_{\ell,\ell,i}$ intended for loudspeaker ℓ, individually processed by all nodes in the neighborhood of node ℓ.

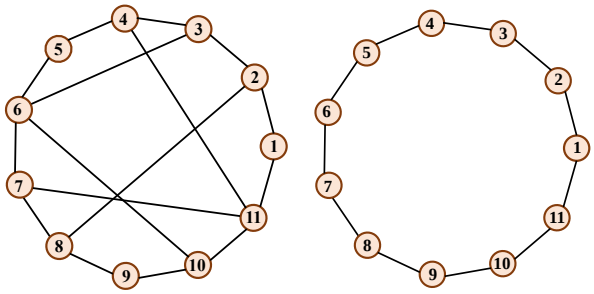

(a) Topology 1. (b) Topology 2.

Fig. 2: Examples of network topologies for distributed system.

The Group diffusion LMS originally defined in [17] allows groups of parameter vectors entries scattered over neighboring nodes, to reach a consensus. We consider using this strategy to estimate the driving signal parameter $d_{\ell,\ell,i}$ in a collaborative manner at each node ℓ based on a consensus reached within each group $\mathcal{G}_\ell \triangleq \{d_{\ell,k,i}\}_{k \in \mathcal{N}_\ell}$ for all $\ell \in \mathcal{N}$. Note that each entry of $\boldsymbol{d}_k$ is individually involved in a group, and:

$$\bigcup_{k=1}^{N} \mathcal{G}_k = \mathcal{G}, \quad \mathcal{G}_k \cap \mathcal{G}_\ell = \emptyset \text{ if } k \neq \ell, \tag{16}$$

with $\mathcal{G}$ the set of all entries of all parameter vectors $\boldsymbol{d}_k$ in the network. We denote by $[\boldsymbol{d}_{k,i}]_{\mathcal{G}_m}$ the entry of $\boldsymbol{d}_{k,i}$ in group $\mathcal{G}_m$ if any. The Group diffusion LMS [17] applied to problem (10) leads to the proposed distributed non-convex decomposition wave-domain ANC via Group diffusion algorithm (DNCD-G):

$$\boldsymbol{\psi}_{k,i} = \boldsymbol{d}_{k,i-1} - \mu \nabla J_k(\boldsymbol{d}_{k,i-1}) \tag{17}$$

$$[\boldsymbol{d}_{k,i}]_{\mathcal{G}_m} = \sum_{\ell \in \mathcal{N}_k} a_{\ell k,m} [\boldsymbol{\psi}_{\ell,i}]_{\mathcal{G}_m} \tag{18}$$

with $\nabla J_k(\boldsymbol{d}_{k,i-1}) = \boldsymbol{Z}_k \boldsymbol{e}_{k,i-1}$ the gradient of $J_k(\boldsymbol{d}_k)$ defined by (11) with respect to $\boldsymbol{d}_k^{\mathrm{H}}$, $\mu = \mu_0 / \|\boldsymbol{Z}_k\|^2$, with $\mu_0 > 0$ the normalized step-size, and $\|\cdot\|$ the ℓ_2-norm of its vector or matrix argument. The coefficients $a_{\ell k,m}$ are usually treated as free weighting parameters to be chosen by the designer. It is sufficient to select them as non-negative convex combination coefficients satisfying:

$$a_{\ell k,m} \geq 0, \quad \sum_{\ell \in \mathcal{N}_k} a_{\ell k,m} = 1, \tag{19a}$$

$$a_{\ell k,m} = 0 \quad \text{if } \ell \notin \mathcal{N}_k \text{ or } \ell, k \notin \mathcal{G}_m. \tag{19b}$$

where condition (19b) means that we can only combine entries which are in a same group. The selection of $a_{\ell k,m}$, e.g., the static combination rules [12] and the adaptive combination rules [11], has a substantial effect on the algorithm's efficacy.

IV. Simulations

The effectiveness of the proposed DNCD-G algorithm is validated by comparing its performance to that of the distributed normalized wave-domain algorithm based on the diffusion LMS (DNWD-G) [10] and its centralized counterpart (CNWD) [18] both in free and reverberant environments.

Consider the image-source approach for generating the reverberant field of the room [23]. We considered the circular control field depicted in Figure 1 with radius R_1 equal to 0.5 meter, and a 2D point-wise noise source located at $(2, 0^\circ)$, with

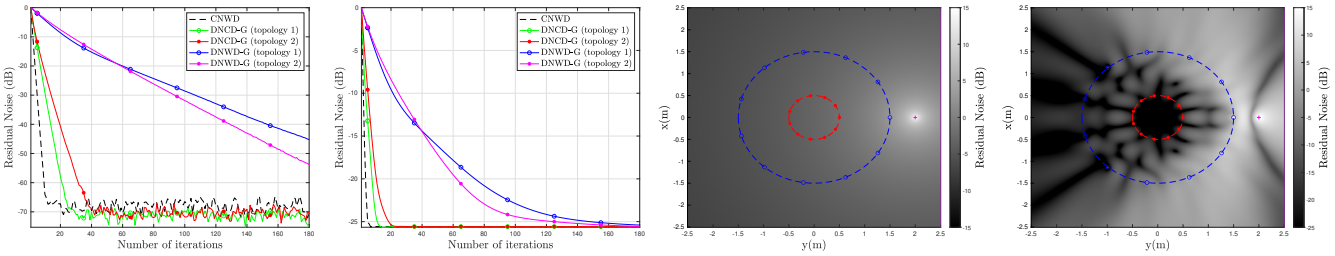

(a) (b) (c) (d)

Fig. 3: Comparison of the residual noise in free field. (a) Residual noise on the boundary of control area; (b) Residual noise inside the control area; (c) Primary noise field; (d) Noise cancellation performance of topology 1 after 20 iterations.

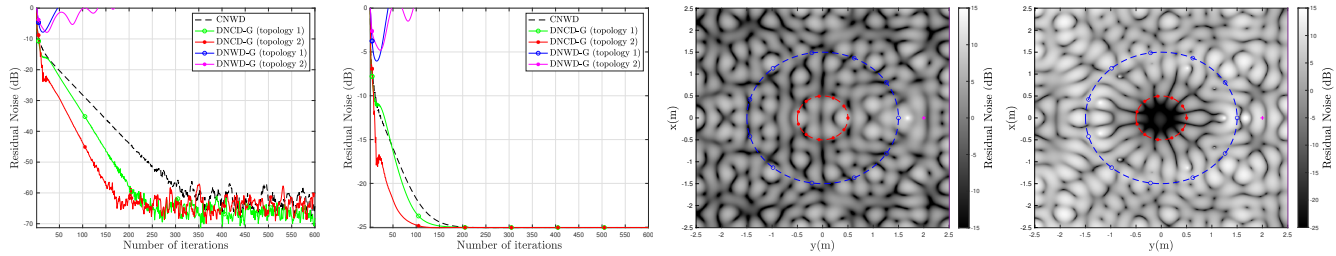

(a) (b) (c) (d)

Fig. 4: Comparison of the residual noise in reverberant field. (a) Residual noise on the boundary of control area; (b) Residual noise inside the control area; (c) Primary noise field; (d)Noise cancellation performance of topology 1 after 80 iterations.

TABLE I: Comparison of computational complexity

Algorithms	Additions	Multiplications
CNWD	$2N \times (N_{\mathcal{F}}^{+} + N_{\mathcal{M}}^{+}) + (N \times N) \times \mathcal{F}$	$2N \times (N_{\mathcal{F}}^{\times} + N_{\mathcal{M}}^{\times}) + [N \times (N+1)] \times \mathcal{F}$
DNCD-G	$2\lvert\mathcal{N}_k\rvert \times (N_{\mathcal{F}}^{+} + N_{\mathcal{M}}^{+}) + (\lvert\mathcal{N}_k\rvert \times \lvert\mathcal{N}_k\rvert) \times \mathcal{F}$	$2\lvert\mathcal{N}_k\rvert \times (N_{\mathcal{F}}^{\times} + N_{\mathcal{M}}^{\times}) + [\lvert\mathcal{N}_k\rvert \times (2\lvert\mathcal{N}_k\rvert + 1)] \times \mathcal{F}$
DNWD-G	$2\lvert\mathcal{N}_k\rvert \times (N_{\mathcal{F}}^{+} + N_{\mathcal{M}}^{+}) + (\lvert\mathcal{N}_k\rvert \times \lvert\mathcal{N}_k\rvert) \times \mathcal{F}$	$2\lvert\mathcal{N}_k\rvert \times (N_{\mathcal{F}}^{\times} + N_{\mathcal{M}}^{\times}) + [\lvert\mathcal{N}_k\rvert \times (\lvert\mathcal{N}_k\rvert + 2)] \times \mathcal{F}$

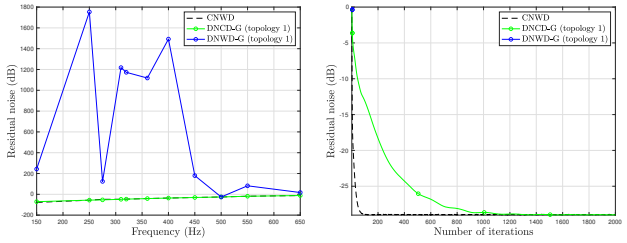

(a) (b)

Fig. 5: Comparison of the multi-frequency noise reduction performance in free field. (a) Residual noise inside the control region on frequency bin after 2000 iterations; (b) Residual noise inside the control region over iterations.

a magnitude of 15 and a frequency of 500 Hz. The ceiling and floor of the 6meters × 6meters rectangular room were represented with fully absorbing surfaces. On the contrary, the reflection coefficients of the remaining side walls were set to 0.75. We set the modes in (1) to $\rho \in [-5, 5]$ based on [19], with $2S+1 = 11$ equiangularly-equipped microphones located on the boundary for measuring the residual signal. The secondary sound source was created with $Q = 11$ loudspeakers arranged in a circle of radius R_2 equal to 1.5 meter.

We simulated signal-task ANC networks with the two topologies depicted in Figures 2(a) and 2(b). We adopted the uniform rule to determine the value of the coefficients $\{a_{\ell k,m}\}$, specifically: $a_{\ell k,m} = \frac{1}{|\mathcal{N}_k|}$, if $\ell \in \mathcal{N}_k$ and $\ell, k \in \mathcal{G}_m$; otherwise, $a_{\ell k,m} = 0$. For both free and reverberant fields, a window length of 3200 samples and a sampling rate of 8 kHz were employed. The microphone signal at each node was characterized by a SNR of 40 dB with zero-mean white Gaussian noise added. We set the step size to $\mu_0 = 8$ for all nodes in the comparison of the performance of the centralized algorithm and its distributed counterparts. In order to evaluate the algorithms, we considered two criteria for the performance comparison, i.e., the residual noise on the boundary of control area $E_{\mathrm{b}}(i) \triangleq 10\log_{10}\frac{\sum_n |e_n(i)|^2}{\sum_n |e_n(0)|^2}$ and the residual noise inside the control area $E_{\mathrm{in}}(i) \triangleq 10\log_{10}\frac{\sum_{\boldsymbol{r}} |e_{\mathrm{in},\boldsymbol{r}}(i)|^2}{\sum_{\boldsymbol{r}} |e_{\mathrm{in},\boldsymbol{r}}(0)|^2}$, respectively, where $e_n(i)$ and $e_{\mathrm{in},\boldsymbol{r}}(i)$ denoted the residual signals observed at the n-th microphone and the arbitrary position $\boldsymbol{r}$ inside the control area at time instant i, respectively.

Figures 3 and 4 illustrate the noise cancellation behavior of the proposed DNCD-G algorithm with the two network topologies, in the free field and reverberant environment, respectively. Figures 3(a) and 4(a) represent the residual noise measured by the 11 microphones. Figures 3(b) and 4(b) illustrate the residual noise measured at 1296 points uniformly sampled throughout the control region. With topology 1, the residual noise fields are shown in Figures 3(d) for free field and 4(d) for reverberant field in comparison to the primary noise fields (Figures 3(c) and 4(c)), where the proposed DNCD-G algorithm executes for 20 and 80 iterations, respectively.

After a number of iterations, in the free field, both distributed algorithms DNCD-G and DNWD-G reached a steady state comparable to their centralized counterpart (CNWD). However, the DNCD-G algorithm achieved improved convergence performance with a faster convergence rate compared to the DNWD-G algorithm. In the reverberant field, only the DNCD-G and CNWD attained similar steady-state

misadjustment, while DNWD-G diverged. Moreover, DNCD-G over topology 2 performed better in reverberant fields. This is most likely because a larger number of node connections will result in longer estimated filter lengths on nodes, which will influence the algorithm's convergence speed.

Figure 5 depicts multi-frequency noise reduction performance in the control zone in free field, where a single noise source was generated by the combination of $H = 11$ dominant narrowband components located at $(2, 0^\circ)$. Each frequency bin $f_h, h = 1, \ldots, H$, had the same pressure magnitude of 15, with values of $\{150, 250, 275, 310, 320, 360, 400, 450, 500, 550, 650\}$. In order to ensure the performance of the algorithms, we set the corresponding step size μ_0 for each frequency point, that is, $\{0.9, 8, 8, 8, 8, 8, 8, 8, 8, 8, 8\}$ for CNWD and $\{2, 0.9, 0.9, 8, 8, 8, 8, 8, 8, 0.9, 0.9\}$ for distributed counterparts. Other experiment settings were identical to the ANC task for the single-frequency signal in the free field. Validation of the proposed algorithm was over the network topology of 1. Figure 5(a) demonstrates that, after 2000 iterations, the DNCD-G performs comparably to the CNWD across all frequency bins. In Figure 5(b), it is evident that the DNCD-G operates in a steady state comparable to its centralized version, while the DNWD-G diverges swiftly after execution.

We further conducted an analysis of the computational complexity of the wave domain-based ANC methods, as shown in Table I. We evaluated the computational load at each iteration on the centralized processor for centralized algorithms and on the processor of each node k for distributed algorithms. The computational complexity was divided into three components: the FFT operation, wave-domain transform, and wave-domain processing. The parameter $\mathcal{F}$ in this table represents the number of fast Fourier transform (FFT) operations with $N_{\mathcal{F}}^{+} \triangleq \mathcal{F}\log_2\mathcal{F}$ and $N_{\mathcal{F}}^{\times} \triangleq \frac{\mathcal{F}}{2}\log_2\mathcal{F}$ as the complex additions and multiplications numbers, respectively. $N_{\mathcal{M}}^{+}$ and $N_{\mathcal{M}}^{\times}$ represent the complex additions and multiplications numbers in wave-domain transform, respectively. The results presented in Table I demonstrate that the proposed distributed method effectively distributes the computational load among to the processors of each node, thereby reducing the communication load compared to the centralized approach. In wave-domain processing, the proposed DNCD-G method has marginally greater computational complexity in terms of multiplications than the DNWD-G method. This improvement in load distribution enhances the system's scalability and controls the performance versus computational complexity trade-off.

V. Conclusion

In this paper, a distributed wave-domain ANC algorithm was proposed based on the convex sum of non-convex quadratic costs. The optimization problem was proposed with the Group diffusion LMS to ensure the consistency of the driving signal parameters locally estimated by nodes and their neighbors. This approach enables a distributed implementation with scalability and minimal computational cost. Simulation results in free field and reverberant environments and computational complexity analysis validated the proposed algorithm. Our future work will consist of the convergence analysis the DNCD-G algorithm, and extension to multi-channel and real-world environments.

REFERENCES

[1] T. Münzel, T. Gori, W. Babisch, and M. Basner, "Cardiovascular effects of environmental noise exposure," *Eur. Heart J.*, vol. 35, no. 13, pp. 829–836, 2014.

[2] S. J. Elliott and P. A. Nelson, "Active noise control," *IEEE Signal Process. Mag.*, vol. 10, no. 4, pp. 12–35, Oct. 1993.

[3] H. c. Chen, P. Samarasinghe, T. D Abhayapala, and W. Zhang, "Spatial noise cancellation inside cars: Performance analysis and experimental results," in *Proc. IEEE WASPAA*. IEEE, 2015, pp. 1–5.

[4] H. c. Chen, P. Samarasinghe, and T. D. Abhayapala, "In-car noise field analysis and multi-zone noise cancellation quality estimation," in *Proc. Asia-Pacific Signal Inf. Process. Ass. Ann. Sum. and Conf. (APSIPA ASC)*. IEEE, 2015, pp. 773–778.

[5] J. Benesty and D. R. Morgan, "Frequency-domain adaptive filtering revisited, generalization to the multi-channel case, and application to acoustic echo cancellation," in *Proc. IEEE Int. Conf. Acoust., Speech, Signal Process. (ICASSP)*, Istanbul, Turkey, Jun. 2000, vol. 2, pp. II789–II792.

[6] M. Bouchard and S. Quednau, "Multichannel recursive-least-square algorithms and fast-transversal-filter algorithms for active noise control and sound reproduction systems," *IEEE/ACM Trans. Audio, Speech, Lang. Process.*, vol. 6, no. 5, pp. 606–618, Sep. 2000.

[7] H. Buchner, S. Spors, and W. Kellermann, "Wave-domain adaptive filtering: acoustic echo cancellation for full-duplex systems based on wave-field synthesis," in *Proc. IEEE Int. Conf. Acoust., Speech, Signal Process. (ICASSP)*, Montreal, Quebec, Canada, May 2004, vol. 4, pp. iv117–iv120.

[8] C. Antonanzas, M. Ferrer, A. Gonzalez, M. de Diego, and G. Piñero, "Diffusion algorithm for active noise control in distributed networks," in *Proc. Int. Cong. Sound Vib.*, 2015.

[9] M. Ferrer, M. de Diego, G. Piñero, and A. Gonzalez, "Active noise control over adaptive distributed networks," *Signal Process.*, vol. 107, no. 20, pp. 82–95, 2015.

[10] Y. Dong, J. Chen, and W. Zhang, "Distributed wave-domain active noise control based on the diffusion adaptation," *IEEE/ACM Trans. Audio, Speech, Lang. Process.*, vol. 28, pp. 2374–2385, 2020.

[11] C. G. Lopes and A. H. Sayed, "Diffusion least-mean squares over adaptive networks: Formulation and performance analysis," *IEEE Trans. Signal Process.*, vol. 56, no. 7, pp. 3122–3136, July 2008.

[12] A. H. Sayed, "Diffusion adaptation over networks," in *Academic Press Library in Signal Processing*, vol. 3, pp. 323–454. Elsevier, 2014.

[13] J. Chen, C. Richard, and A. H. Sayed, "Diffusion LMS over multitask networks," *IEEE Trans. Signal Process.*, vol. 63, no. 11, pp. 2733–2748, Jun. 2015.

[14] M. O'Connor, W. B. Kleijn, and T. Abhayapala, "Distributed sparse mvdr beamforming using the bi-alternating direction method of multipliers," in *Proc. IEEE Int. Conf. Acoust., Speech, Signal Process. (ICASSP)*, 2016, pp. 106–110.

[15] S. Gade and N. H. Vaidya, "Distributed optimization of convex sum of non-convex functions," *arXiv preprint arXiv:1608.05401*, 2016.

[16] K. Hu, D. Jin, W. Zhang, and J. Chen, "Distributed optimization of quadratic costs with a group-sparsity regularization via pdmm," in *Proc. Asia-Pacific Signal Inf. Process. Ass. Ann. Sum. and Conf. (APSIPA ASC)*, 2018, pp. 1825–1830.

[17] J. Chen, S. K. Ting, C. Richard, and A. H. Sayed, "Group diffusion LMS," in *Proc. IEEE Int. Conf. Acoust., Speech, Signal Process. (ICASSP)*, Shanghai, China, March 2016.

[18] J. Zhang, T. D. Abhayapala, W. Zhang, P. N. Samarasinghe, and S. Jiang, "Active noise control over space: A wave domain approach," *IEEE/ACM Trans. Audio, Speech, Lang. Process.*, vol. 26, no. 4, pp. 774–786, Apr. 2018.

[19] D. B. Ward and T. D. Abhayapala, "Reproduction of a plane-wave sound field using an array of loudspeakers," *IEEE/ACM Trans. Audio, Speech, Lang. Process.*, vol. 9, no. 6, pp. 697–707, Sep. 2001.

[20] T. Betlehem and T. D. Abhayapala, "Theory and design of sound field reproduction in reverberant rooms," *J. Acoust. Soc. Am.*, vol. 117, no. 4, pp. 2100–2111, Apr. 2005.

[21] S. Boyd and L. Vandenberghe, *Convex Optimization*, Cambridge University Press, 2004.

[22] A. H. Sayed, "Adaptation, learning, and optimization over networks," *Foundations and Trends in Machine Learning*, vol. 7, no. 4-5, pp. 311–801, 2014.

[23] J. B. Alien, "Image method for efficiently simulating small-room acoustics," *J. Acoust. Soc. Am.*, vol. 65, no. 4, pp. 943–950, 1979.